THE JOURNAL OF BIOLOGICAL CHEMISTRY VOL. 287, NO. 14, pp. 11303–11311, March 30, 2012

Pannexin 1, an ATP Release Channel, Is Activated by Caspase Cleavage of Its Pore-associated C-terminal Autoinhibitory Region*[S]◆

Received for publication, November 14, 2011, and in revised form, February 3, 2012 Published, JBC Papers in Press, February 6, 2012, DOI 10.1074/jbc.M111.323378

Joanna K. Sandilos[‡], Yu-Hsin Chiu[‡], Faraaz B. Chekeni[‡§], Allison J. Armstrong[§¶], Scott F. Walk[§¶], Kodi S. Ravichandran[§¶‖], and Douglas A. Bayliss[‡1]

From the [‡]Department of Pharmacology, [§]Beirne B. Carter Center for Immunology Research, [¶]Center for Cell Clearance, and [‖]Department of Microbiology, University of Virginia, Charlottesville, Virginia 22908

Background: Pannexin 1 is activated by caspase cleavage of its C-terminal tail during apoptosis.
Results: Cleavage removes a critical adjacent region to activate membrane-associated PANX1; activation requires dissociation of the C terminus from the pore.
Conclusion: An intrinsic inhibitory interaction between the C terminus and the pore constrains PANX1 activity.
Significance: PANX1 activation is caused by disruption of C-terminal-mediated inhibition.

Pannexin 1 (PANX1) channels mediate release of ATP, a "find-me" signal that recruits macrophages to apoptotic cells; PANX1 activation during apoptosis requires caspase-mediated cleavage of PANX1 at its C terminus, but how the C terminus inhibits basal channel activity is not understood. Here, we provide evidence suggesting that the C terminus interacts with the human PANX1 (hPANX1) pore and that cleavage-mediated channel activation requires disruption of this inhibitory interaction. Basally silent hPANX1 channels localized on the cell membrane could be activated directly by protease-mediated C-terminal cleavage, without additional apoptotic effectors. By serial deletion, we identified a C-terminal region just distal to the caspase cleavage site that is required for inhibition of hPANX1; point mutations within this small region resulted in partial activation of full-length hPANX1. Consistent with the C-terminal tail functioning as a pore blocker, we found that truncated and constitutively active hPANX1 channels could be inhibited, in *trans*, by the isolated hPANX1 C terminus either in cells or when applied directly as a purified peptide in inside-out patch recordings. Furthermore, using a cysteine cross-linking approach, we showed that relief of inhibition following cleavage requires dissociation of the C terminus from the channel pore. Collectively, these data suggest a mechanism of hPANX1 channel regulation whereby the intact, pore-associated C terminus inhibits the full-length hPANX1 channel and a remarkably well placed caspase cleavage site allows effective removal of key inhibitory C-terminal determinants to activate hPANX1.

Pannexins are a relatively recently identified family of channels, distantly related by sequence to the gap junction-forming mammalian connexins and invertebrate innexins, with similar putative transmembrane topology (1, 2). Initial expectations that pannexins might also incorporate into intercellular gap junctions have given way to current views that they instead form membrane channels (3). Among the three members of the pannexin family, pannexin 1 (PANX1)[2] has garnered the most attention. PANX1 forms a plasma membrane ion channel with a large single channel conductance (~500 picosiemens) and a pore that permits permeation by small molecules up to 1 kDa in size (2, 4). PANX1 channels allow efflux of signaling nucleotides, ATP and UTP, and influx of specific dyes that are used to visualize cells undergoing apoptosis (*e.g.* Yo-Pro, To-Pro) (5, 6).

Several distinct mechanisms have been suggested for modulation of PANX1 activity in association with different physiological processes. For example, mPanx1 channels can be activated by mechanical stress (7), and there is evidence that high extracellular K^+ activates Panx1 in rat neurons and astrocytes as part of the inflammasome (8). mPanx1 is also activated by purinergic receptors, where extracellular ATP binding to P2X and P2Y receptors supports "ATP-induced ATP release" (9). In addition, mPanx1 activation by α1-adrenoreceptor stimulation in vascular smooth muscle cells enhances norepinephrine-mediated vasoconstriction (10). Of particular relevance to this work, we recently showed that PANX1 channels are selectively activated in apoptotic cells (5); this PANX1 activation is necessary for release of ATP and UTP, which serve as chemoattractant "find-me" signals for monocyte/macrophage recruitment toward dying cells and subsequent corpse clearance (6). Our work was recently verified using Panx1 knock-out mice, in which apoptotic $Panx1^{-/-}$ thymocytes were found to be deficient in dye uptake, ATP release, and recruitment of peritoneal macrophages (11).

* This work was supported, in whole or in part, by National Institutes of Health Fellowship F30HL09640 (to F. B. C.) and Grants GM064709 (to K. S. R.) and NS033583 (to D. A. B.). This work was also supported by a Pharmacological Sciences Training Grant T32GM007055 (to J. K. S. and F. B. C.), a predoctoral fellowship from the American Heart Association (PRE223005, to J. K. S.), and a postdoctoral fellowship from American Cancer Society (PF-11-024-01-CCG to A. J. A.).
◆ This article was selected as a Paper of the Week.
[S] This article contains supplemental Figs. S1–S5.
[1] To whom correspondence should be addressed: Dept. of Pharmacology, University of Virginia, 1340 Jefferson Park Ave., 5013 Jordan Hall, Charlottesville VA 22908. Tel.: 434-982-4449; Fax: 434-924-0149; E-mail: bayliss@virginia.edu.

[2] The abbreviations used are: PANX1, pannexin 1; hPANX1, human PANX1; mPanx1, mouse Panx1; Casp3, caspase 3; TEV, tobacco etch virus; TEVp, TEV protease; CBX, carbenoxolone; TCEP, tris(2-carboxyethyl)phosphine; pA/pF, picoamperes per picofarads; Ct, C terminus.

For most forms of modulation, the mechanisms that account for PANX1 activation remain obscure. In apoptotic cells, we found that caspase-mediated cleavage of the C terminus is required for hPANX1 activation (5). This caspase-dependent mechanism for channel regulation not only links cell death signaling pathways directly to corpse clearance, but also presents a previously unknown proteolysis-based channel activation process. In this study, we examine mechanisms by which C-terminal cleavage activates hPANX1 channels. Our data indicate that the C-terminal regions of hPANX1 function to inhibit hPANX1 channels and that removal by cleavage of key determinants immediately downstream of the caspase site allows dissociation of the C terminus from the channel pore, relieving C-terminally mediated inhibition.

EXPERIMENTAL PROCEDURES

Reagents—TEV protease was purchased from Accelagen and dialyzed into recording solution using 30K centrifugal filters (Millipore). To-Pro-3 dye was obtained from Invitrogen, monoclonal anti-FLAG antibody was obtained from Sigma, and anti-GFP antibody was from Abcam (ab290). Annexin-V-FITC was obtained from BD Biosciences, carbenoxolone was obtained from Fisher, hPANX1 peptide (GKTPMSAEMREE) was obtained from Biomolecules Midwest Inc., purified GST fusion proteins were from Genscript, and TCEP-HCl was obtained from Thermo Scientific. Purified, activated caspase 3 was a gift from G. S. Salvesen; it has been described previously (12).

DNA Constructs—Full-length pEBBhPANX1-FLAG and hPANX1Δ391-FLAG constructs were described previously (5), and pEBBmPanx1-FLAG was generated by PCR cloning mPanx1 cDNA (Open Biosystems) into pEBB-FLAG vector after inserting SpeI and KpnI restriction sites. The TEV protease expression vector was kindly provided by S. R. Ikeda (13). All mutations were performed using QuikChange (Stratagene) and confirmed by sequencing. The PANX1(TEV) constructs were generated by exchanging caspase cleavage sequence (IKMDVVD) with TEV protease cleavage site (ENLYFQG). EGFP-hPANX1Ct was generated by inserting the C-terminal region residues of hPANX1 (residues 299–426) into EGFP-C1 vector (Clontech). GST-hPANXCt-FLAG was generated by inserting residues 299–426 from pEBBhPANX1-FLAG into pGEX-2T (GE Healthcare). Sequential hPANX1 truncation mutants (hPANX1Δ391, -Δ401, and -Δ413) were generated by PCR to introduce a FLAG tag (DYKDDDDK) followed by stop codon at the relevant positions.

Cell Culture and Transfections—HEK293T cells were transfected using Lipofectamine 2000 (Invitrogen). Green fluorescent protein (pEGFP) was co-transfected in a fixed amount of DNA for each transfection within individual experiments. One day after transfection, cells were plated onto poly-L-lysine-coated glass coverslips and kept in a humidified 5% CO_2 atmosphere at 37 °C for 1 h. All recordings were performed within 5 h of plating.

Electrophysiology—Whole cell recordings were obtained at room temperature with 3–5-megaohm borosilicate glass patch pipettes and an Axopatch 200A amplifier (Molecular Devices) in a bath solution composed of 140 mM NaCl, 3 mM KCl, 2 mM $MgCl_2$, 2 mM $CaCl_2$, 10 mM HEPES, and 10 mM glucose (pH 7.3). Internal solution contained 30 mM tetraethylammonium chloride, 100 mM $CsMeSO_4$, 4 mM NaCl, 1 mM $MgCl_2$, 0.5 mM $CaCl_2$, 10 mM HEPES, 10 mM EGTA, 3 mM ATP-Mg, and 0.3 mM GTP-Tris (pH 7.3). Ramp voltage clamp commands were applied at 5-s intervals using the pCLAMP software and a Digidata 1322A digitizer (Molecular Devices). Peak currents were taken at +80 mV and normalized to cell capacitance (*i.e.* current density). Carbenoxolone (CBX)-sensitive current was taken as the difference in peak current before and after CBX application.

Inside-out patch recordings were obtained using 1–2-megaohm patch pipettes with pipette solution containing 140 mM NaCl, 3 mM KCl, 10 mM HEPES (pH 7.3). Gigaohm seals were obtained in the bath solution described above, and immediately before patches were pulled, the bath solution was exchanged for a calcium-free patch recording solution containing 150 mM CsCl, 5 mM EGTA, 1 mM $MgCl_2$, 10 mM HEPES (pH 7.3).

Flow Cytometry—HEK293T cells were incubated in medium containing 1 μM To-Pro-3 dye. Cells were washed in PBS and resuspended in either PBS, 0.5% BSA or binding buffer for annexin-V staining. Dye uptake and cell surface staining were assessed by flow cytometry.

Immunofluorescence—HEK293T cells were transfected as described previously and plated on poly-L-lysine-coated coverslips 18 h later. Cells were fixed with 4% paraformaldehyde and mounted onto gelatin-subbed slides. GFP fluorescence images were captured with a Zeiss LSM150 confocal microscope and analyzed using the IPLab software (BioVision Technologies).

Cell Surface Biotinylation—Cell surface biotinylation studies were carried out in HEK293T cells transiently transfected with hPANX1 channels. To prevent diffusion of biotin reagents through open hPANX1 channels, cells were treated with 50 μM CBX at 4 °C for 15 min before biotin labeling. CBX-pretreated cells were labeled with 1 mg/ml EZ-Link Sulfo-NHS-Biotin™ reagent (Thermo Scientific) in the presence of CBX (50 μM) in PBS at 4 °C for 1 h. Biotin-labeled cells were incubated in cold PBS containing 100 mM glycine for an additional 20 min at 4 °C to quench the reaction. Cells were lysed in PBS containing 1% Triton X-100 (Sigma-Aldrich) and a mixture of protease inhibitors (Sigma-Aldrich). The biotinylated proteins from the cell surface were recovered from the remainder of the lysates by incubating with immobilized streptavidin-agarose beads (Thermo Scientific) at 4 °C for 2 h. To demonstrate cell surface expression of hPANX1Δ371, transfected cells were labeled with biotin as described above, and hPANX1 proteins were immunoprecipitated by using anti-FLAG M2 agarose (Sigma-Aldrich). Immunoprecipitated hPANX1 proteins were eluted with FLAG peptide (Sigma-Aldrich), and the biotinylated fraction was further immunoprecipitated using streptavidin-agarose, as described above.

Data Analysis—Data are presented as mean ± S.E. Statistical analysis was by χ^2 analysis, Student's *t* test, or analysis of variance, with post hoc comparisons made using a Bonferroni-corrected *t* test; differences between groups were considered significant if $p < 0.05$.

RESULTS

C-terminal Cleavage Activates Plasma Membrane hPANX1 Channels, Independent of Apoptosis—Native PANX1 channels expressed in human T cells are silent under basal conditions and become activated by various apoptotic stimuli (*e.g.* ultraviolet irradiation or Fas ligation) (5). Because a caspase cleavage site was identified within the C-terminal tail of hPANX1 and mutation of this site precludes hPANX1 activation, caspase-dependent cleavage of the channel C terminus was proposed as a mechanism for hPANX1 activation during apoptosis (5). However, contributions from other cell death mediators to hPANX1 activation could not be excluded.

To test whether caspases can directly activate hPANX1, without the full apoptotic signaling cascade, we obtained whole cell patch clamp recordings from Jurkat cells using pipettes that contained purified, activated caspase 3 (Casp3; Fig. 1*A*). In recordings from apparently "healthy" cells, small currents were obtained immediately upon whole cell access that increased progressively with time, presumably reflecting the time required for Casp3 to reach effective concentrations in the cell; we did not see time-dependent activation of current in control recordings with heat-inactivated Casp3. The Casp3-activated current appeared to be carried by native hPANX1 channels because it was completely eliminated by CBX, an hPANX1 channel blocker, and displayed a current-voltage (*I*-V) relationship identical to that previously described for hPANX1 (5). The CBX-sensitive current density was 54.8 ± 19.1 pA/pF in Casp3 dialyzed cells but only 5.8 ± 2.3 pA/pF in control cells ($n = 4$ and 6, $p < 0.05$). It is important to note that the Jurkat cells that showed this caspase-dependent increase in hPANX1 currents did not display morphological properties characteristic of apoptosis (*e.g.* blebbing, cell shrinking, etc.). These data suggest that Casp3 can activate native hPANX1 channels in Jurkat cells directly, without other apoptosis-associated morphological events.

To test whether cleavage-mediated activation of hPANX1 can occur when the C terminus is cleaved by another protease (thereby completely eliminating the need for caspases and apoptosis), we generated an hPANX1 variant that substitutes a tobacco etch virus protease (TEVp) site at the C-terminal caspase cleavage site (Fig. 1*B*), maintaining both the channel length and the position of the cleavage site. We made whole cell patch clamp recordings in HEK293T cells co-expressing hPANX1(TEV) and TEVp and observed robust CBX-sensitive hPANX1 currents, identical to those recorded in apoptotic Jurkat cells (4). Current activation required the presence of both the mutant channel containing the TEV cleavage site and the TEV protease because neither hPANX1(TEV) alone nor wild type hPANX1 co-expressed with TEVp generated currents (Fig. 1*C*). The absence of CBX-sensitive current in cells transfected with hPANX1(TEV) alone or with wild type hPANX1 and TEVp was not due to a failure of expression or membrane localization; cell surface biotinylation assays indicate that both hPANX1(TEV) and wild type hPANX1 were present on the plasma membrane at comparable levels (Fig. 1*C*, *inset*). The absence of FLAG immunoreactivity in cells co-expressing hPANX1(TEV) and TEVp confirmed TEVp-mediated cleavage of that channel and removal of the FLAG epitope from the extreme C terminus. Again, we saw no obvious morphological features of apoptosis in cells chosen for these recordings. As an independent approach, we used flow cytometry to simultaneously measure To-Pro-3 uptake as a surrogate for hPANX1 activation and annexin-V staining to assess apoptosis. As depicted in Fig. 1*D*, To-Pro-3 permeability was clearly enhanced in HEK293T cells co-expressing hPANX1(TEV) together with TEVp as compared with cells expressing wild type hPANX1 and TEVp (mean fluorescence intensity: 788 ± 68 *versus* 165 ± 9, $p < 0.001$). Importantly, the increased To-Pro-3 uptake was not accompanied by annexin-V staining. These data indicate that C-terminal cleavage is sufficient for hPANX1 activation, which can be functionally separated from apoptosis.

To determine whether cleavage-mediated activation can occur with hPANX1 channels that are already localized to the plasma membrane, inside-out patches were pulled from HEK293T cells transfected with either wild type hPANX1 or hPANX1(TEV), and purified active proteases were added to the bath. As shown in Fig. 1*F*, CBX-sensitive hPANX1-like currents were generated by adding Casp3 to patches from wild type hPANX1-expressing cells or by adding TEVp to patches from hPANX1(TEV)-expressing cells (after ~10 min of protease application). There was no current activation when the proteases were applied to patches containing channels that did not include the cognate cleavage site (Fig. 1, *E* and *F*). The *I*-V relationships of these currents were identical to those from truncated hPANX1 channels recorded in this configuration (supplemental Fig. S1). Collectively, these data indicate that C-terminal cleavage can activate plasma membrane hPANX1 channels, without the need for additional signaling mediators.

The Caspase Cleavage Site in hPANX1 Is Located Immediately Upstream of a Crucial C-terminal Regulatory Region—In light of these results, we sought channel-intrinsic determinants and mechanisms by which the hPANX1 C terminus modulates channel function. We previously showed that an hPANX1 construct truncated just upstream of the caspase cleavage site is constitutively active (hPANX1Δ371), whereas full-length human PANX1 is basally inactive (5). To identify regions downstream of Gly-371 that are required for channel inhibition, we generated a panel of serially truncated hPANX1 constructs (Fig. 2*A*). Remarkably, we saw no basal CBX-sensitive current in any of the longer truncation mutants (Fig. 2*B*; hPANX1Δ391, -Δ401, or -Δ413), although all three were expressed and present on the plasma membrane at even higher levels than the highly active hPANX1Δ371 construct (Fig. 2*C*). We suspect that overall low levels of hPANX1Δ371 expression reflect a negative selection for cells with large hPANX1 conductance because we generally observe fewer viable cells after transfection with this construct. Because none of the longer C-terminal truncation mutants showed constitutive activity, these data indicate that a small region between the caspase site and Glu-391 is necessary to maintain the inhibited state of hPANX1. Consistent with this, we found that application of purified Casp3 to the cytoplasmic face of an inside-out patch containing hPANX1Δ391 was able to evoke hPANX1 channel activity (Fig. 2*B*, *inset*). These data demonstrate that hPANX1 can be truncated up to

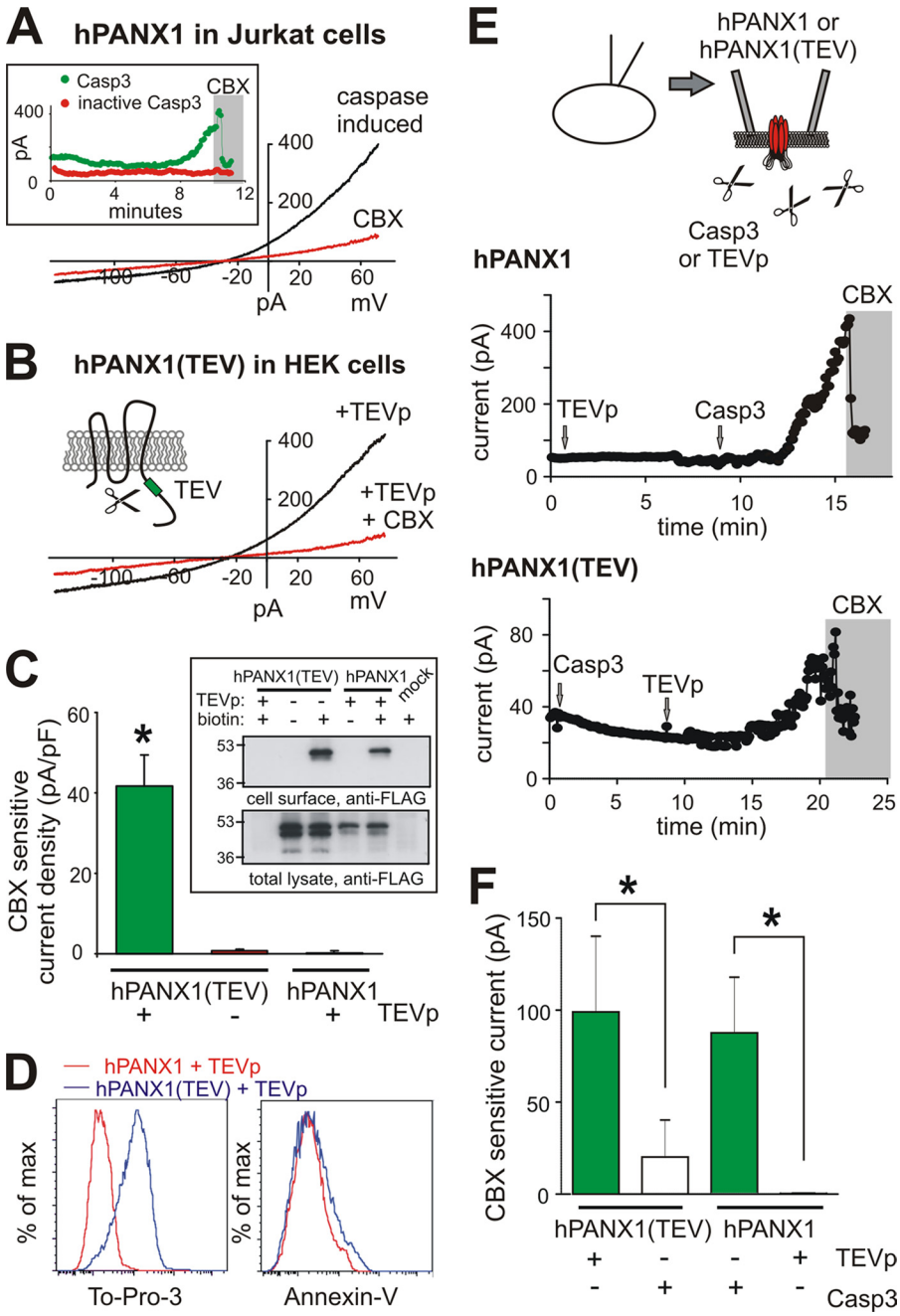

FIGURE 1. **C-terminal cleavage activates membrane-associated hPANX1 channels, independent of apoptosis.** *A*, a CBX-sensitive current with *I*-V properties characteristic of hPANX1 was observed in Jurkat cells recorded under whole cell voltage clamp conditions with pipettes containing purified, activated Casp3 (400 nM). *Inset*, time series of peak current shows that the current developed slowly following whole cell access with pipettes containing active Casp3, but not with those containing heat-inactivated Casp3. *B*, when co-transfected with TEVp in HEK293T cells, hPANX1(TEV) generated robust whole cell CBX-sensitive currents with *I*-V properties characteristic of hPANX1. *Inset*, schematic of the hPANX1(TEV) construct with TEV protease site substituted for caspase site. *C*, averaged data (± S.E.) showing enhanced CBX-sensitive current in cells expressing both hPANX1(TEV) and TEVp, but not in those expressing hPANX1(TEV) alone or wild type channels with TEVp. *, $p < 0.001$. *Inset*, whole cell lysate and avidin pulldowns of biotinylated wild type hPANX1 and hPANX1(TEV). Note the surface localization of wild type and hPANX1(TEV) channels and loss of immunoreactivity to the C-terminal FLAG epitope when hPANX1(TEV) was co-expressed with TEVp. Data are representative of two independent experiments; *mock* indicates transfection with empty vector. *D*, TEVp expression induced To-Pro-3 dye uptake in HEK293T cells co-transfected with hPANX1(TEV) (*blue*) but not with wild type hPANX1 constructs (*red*); dye-loaded cells were not apoptotic, as indicated by the absence of annexin-V staining. *% of max*, percentage of maximum. *E*, the schematic depicts inside-out patch configuration with cytosolic face exposed to the bath solution containing Casp3 or TEVp. *Upper* and *lower graphs*, peak currents in inside-out patches from HEK293T cells expressing wild type hPANX1 (*upper graph*) or the hPANX1(TEV) construct (*lower graph*). The point of application of TEVp and caspase under stop flow conditions is indicated by *arrows*; the time during which CBX was superfused over the patch is indicated by the *gray shading*. *F*, CBX-sensitive current was induced by TEVp only in patches from cells expressing hPANX(TEV) and by Casp3 only in patches containing wild type PANX1. *, $p < 0.05$.

residue Glu-391 and still retain characteristics of a full-length channel (*i.e.* membrane expression and activation by cleavage at C-terminal caspase site). Because removal of the 12 residues immediately downstream of the caspase cleavage site is necessary for constitutive channel activity, we directed our focus on this amino acid sequence.

We first noted that despite strong overall sequence identity between mouse and human PANX1 (87%), there is an especially

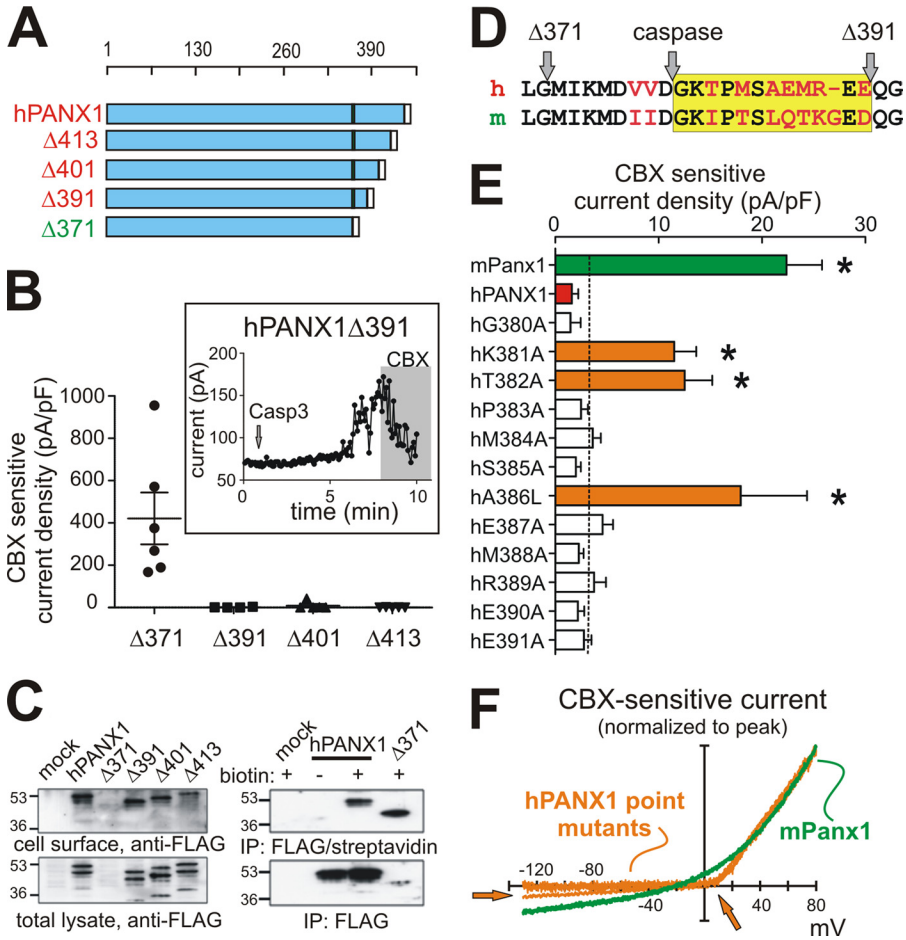

FIGURE 2. **A C-terminal region immediately downstream of caspase cleavage site is essential for hPANX1 channel inhibition.** *A*, schematic of hPANX1 C-terminal deletion constructs; the *white box* indicates FLAG epitope on the extreme C terminus, and the *blue band* indicates the caspase cleavage site. *B*, whole cell CBX-sensitive current density recorded from hPANX1 truncation mutants; only hPANX1Δ371 generated current. *Inset*, time series showing activation by Casp3 of basally inactive hPANX1Δ391 channels in inside-out patch. *C*, whole cell lysate and avidin pulldowns of biotinylated wild type hPANX1 and C-terminal truncation mutants (*left*); note that expression and surface localization for all silent truncation mutants was similar to wild type hPANX1 ($n = 3$). The highly active hPANX1Δ371 construct was expressed at lower levels, but could be detected with longer exposures (data not shown) or by performing the avidin pulldown on FLAG immunoprecipitates (*IP*, *right*; $n = 2$); *mock* indicates transfection with empty vector. *D*, alignment of mPanx1 and hPANX1, highlighting nonconserved residues in the critical region downstream of the caspase cleavage site. *E*, CBX-sensitive current density in cells expressing mPanx1, hPANX1, and the indicated point mutations in hPANX1. The upper boundary of the 95% confidence interval for hPANX1 current density is shown as a *dashed line*. *, $p < 0.05$. *F*, *I*-*V* relationships of CBX-sensitive current from mPanx1 and individual activating hPANX1 point mutants (normalized to peak current at +80 mV); note the more pronounced rectification, with little inward current at hyperpolarized potentials, in mutationally activated hPANX1 channels.

high incidence of mismatch in the region encompassing Gly-371 and Glu-391, which contains the caspase site and the critical adjacent region (Fig. 2*D*). Interestingly, we found that full-length mouse Panx1 produces a measurable constitutive current that was significantly greater than the extremely low basal currents from the full-length human channel (Fig. 2*E*). It is important to point out that C-terminal cleavage was capable of activating mouse Panx1, just like the human channel, despite the larger basal currents obtained from the full-length mPanx1 channel. Indeed, we found that TEVp-mediated cleavage of an mPanx1(TEV) construct yielded currents that were substantially greater than those from full-length mPanx1(TEV) and also very similar to those from hPANX1(TEV) following TEVp cleavage (59.7 ± 9.8 pA/pF; *cf.* supplemental Fig. S2 and Fig. 1*C*). In addition, because surface biotinylation of FLAG-tagged channels consistently revealed lower expression of mPanx1, as compared with hPANX1 (supplemental Fig. S3), the greater basal channel activity in full-length mPanx1 is unlikely to be due to differences in expression or trafficking of the species variants.

In light of these observations, we made mutations of the 12 residues immediately downstream of the caspase cleavage site, on the hPANX1 background. Three mutants of hPANX1 (K381A, T382A, and A386L) generated currents comparable with those seen in mPanx1 (Fig. 2*E*). It is noteworthy that although these point mutants generated a substantial current when measured at +80 mV, this current was smaller than seen with the truncated hPANX1Δ371 channel (*cf.* Fig. 2*B*), and the *I*-V characteristics were unlike those seen with mPanx1 or cleavage-activated hPANX1 (Fig. 2*F*). Rather than providing a weakly rectifying current over the entire voltage range, the mutated channels were more strongly rectifying, producing large outward current at depolarized potentials but little to no inward current at hyperpolarized potentials. These results suggest that mutations of several residues within the region immediately distal to the caspase cleavage site can partially relieve

C-terminal inhibition of hPANX1, especially at depolarized potentials. However, the mutated C-terminal region retains the ability to inhibit inward currents at hyperpolarized potentials.

Constitutively Active hPANX1 Channels Can Be Inhibited in trans by C terminus—The region downstream of caspase cleavage is necessary for hPANX1 modulation, but it was unclear whether this amino acid stretch, by itself, was sufficient to confer channel block. To test this, we made whole cell recordings of TEVp-activated hPANX1 channel currents using pipettes containing a synthetic peptide comprising just these 12 amino acids (GKTPMSAEMREE; 100 μM); we found that intracellular dialysis of this peptide had no detectable effect on hPANX1 currents (99 ± 5% of initial CBX-sensitive current, see supplemental Fig. S4). We therefore considered that hPANX1 channel inhibition may require additional, proximal elements within the C terminus. To address this possibility, we generated an N-terminally enhanced green fluorescent protein (EGFP)-tagged expression construct including the entire putative C-terminal tail region encompassing the region from Phe-299 to Cys-426 (denoted hPANX1(Ct)). When co-expressed with constitutively active hPANXΔ371, the C-terminal construct dose dependently inhibited hPANX1 currents (Fig. 3*A*); it also appeared to associate more avidly with the membrane when co-expressed with hPANXΔ371 (supplemental Fig. S5). On the other hand, hPANX1Δ371 currents were not significantly reduced by co-expression of two fluorescently tagged unrelated proteins of similar size (*i.e.* mSpo20 (14) and PLCδ-PH (15)). Likewise, hPANX1Δ371 currents were unaffected by a C-terminal construct that includes a point mutation (hPANX1(Ct)C347S) known to yield constitutive currents in full-length hPANX1 channels (16). Finally, a C-terminal construct truncated at Glu-391 (hPANX1(Ct)Δ391) provided a block of current that was comparable with that seen with the full-length C terminus, consistent with our observation that residues downstream of Glu-391 are not required for C-terminal inhibition of hPANX1 (*cf.* Fig. 2*B*).

We also tested whether direct application of purified hPANX1 C terminus was able to inhibit constitutive currents from a truncated hPANX1 channel in a cell-free system. To this end, we expressed hPANX1(TEV) and recorded macropatch channel currents in the inside-out configuration following application of purified TEVp in the bath solution (Fig. 3*B*). Once patch access was assured and stable currents were generated from the cleaved channel, TEVp was washed out, and either GST or a purified hPANX1 C-terminal GST fusion protein was applied. As shown in Fig. 3, *C* and *D*, the hPANX1 C-terminal GST fusion protein (~20 μM) caused inhibition of hPANX1 currents (n = 4/8 patches) that was never observed with GST, even at twice the concentration (n = 0/7 patches; $p <$ 0.05 by χ^2 analysis). Note that inward currents at hyperpolarized potentials were most prominently inhibited by the hPANX1 C-terminal protein, whereas outward currents at depolarized potentials were unaffected (Fig. 3*E*). Thus, inhibition by the purified C terminus does not completely recapitulate that mediated by the intact C terminus on full-length hPANX1. Interestingly, however, the rectifying voltage dependence of hPANX1 currents observed after reconstitution of the truncated channel with the purified C terminus was reminiscent of that seen in hPANX1

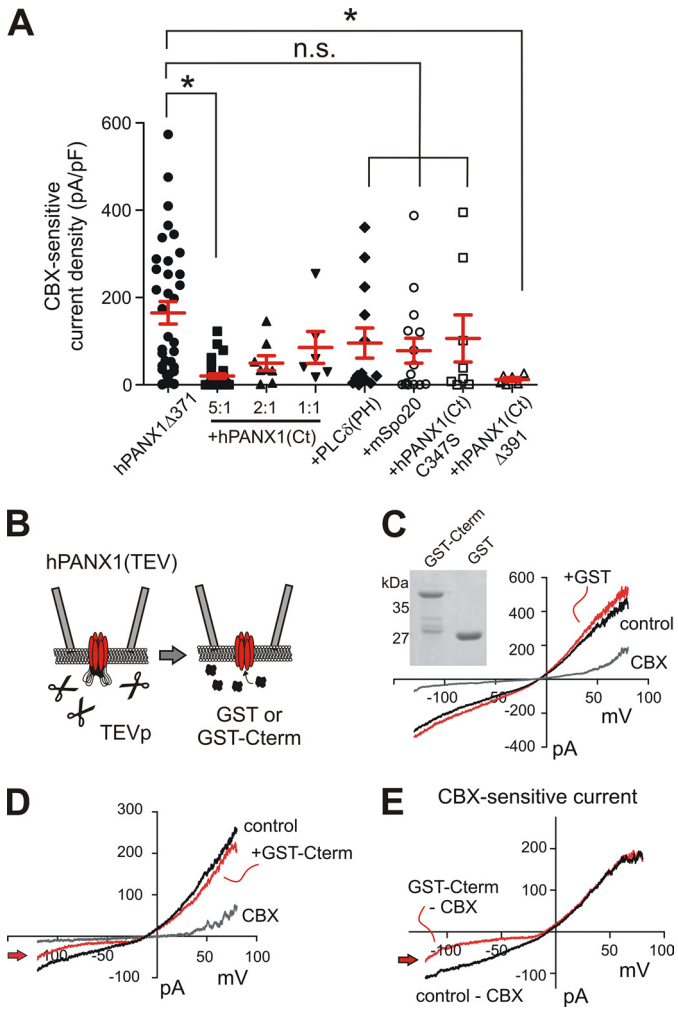

FIGURE 3. **Isolated C terminus can act in *trans* to block hPANX1 current.** *A*, whole cell CBX-sensitive current density from HEK293T cells co-expressing C-terminally truncated and activated hPANX1Δ371 along with the indicated constructs. Both the wild type hPANX1(Ct) and hPANX1(Ct)Δ391 strongly reduced averaged current amplitude and data dispersion, especially when expressed at the highest ratio (5:1), whereas the control constructs did not. *, $p < 0.05$. *n.s.*, not significant. *B*, illustration of inside-out patch recording procedure (*upper left*). GST or purified, hPANX1 C-terminal GST fusion protein (*GST-Cterm*; see *inset* in *panel C* for Coomassie stained gel of GST fusion proteins) was applied to inside-out patches containing TEVp-activated hPANX1(TEV). *C* and *D*, *I-V* relationships of patch currents under the indicated conditions. *control* represents current following activation by TEVp (50 μg/ml); GST (*C*; ~40 μM) and C-terminal GST fusion protein (*D*; ~20 μM) were applied under stop flow conditions before CBX application (50 μM). *E*, *I-V* relationship of CBX-sensitive current before and after C-terminal GST fusion protein application; note that the C-terminal protein only inhibits inward current in the hyperpolarized range (see *arrows*).

channels with C-terminal point mutations; the mutationally activated hPANX1 channels also generated strong outward currents but little inward current (Fig. 2*F*). Thus, the mutated C terminus and isolated C-terminal fragment share the ability to inhibit inward currents at hyperpolarized potentials, but either mutation or *in vitro* reconstitution of the C terminus yields a channel that can pass outward currents at depolarized potentials. Taken together, these data indicate that the C terminus of hPANX1 can act in *trans* to inhibit hPANX1 currents.

Cleavage-mediated Activation Requires Dissociation of C Terminus from hPANX1 Pore—A recent structure-function analysis of mPanx1 provided evidence that the distal region of

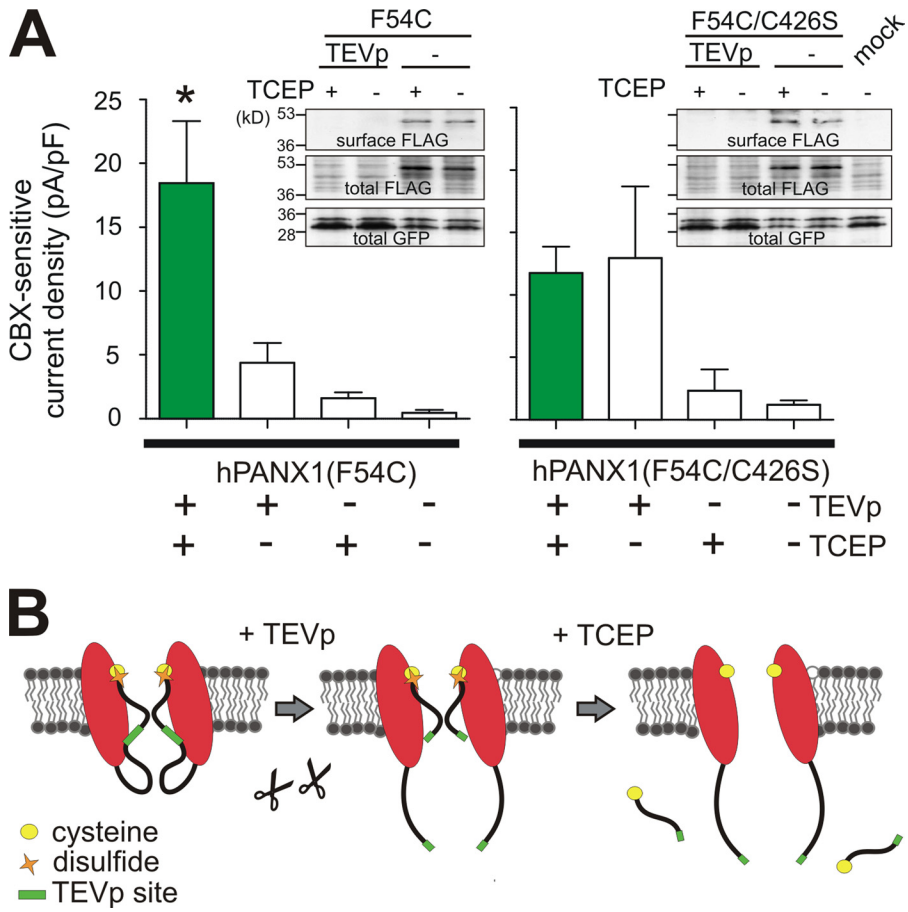

FIGURE 4. **Relief of C-terminal block requires dissociation of C terminus from channel pore.** *A*, whole cell CBX-sensitive current density was determined in HEK293T cells expressing hPANX1(TEV)F54C or hPANX1(TEV)F54C/C426S, with or without TEVp; where indicated, cells were pretreated with the reducing agent, TCEP, prior to recording (500 μM for 2 h). In TEVp-expressing cells, currents were obtained from the cleaved hPANX1(TEV)F54C construct only after TCEP treatment; simultaneous mutation of Cys-426 abolished TCEP sensitivity of the truncated, F54C-mutated channel. *, $p < 0.05$. *Insets*, whole cell lysate and avidin pulldowns of biotinylated F54C and F54C/C426S channels, with or without TCEP pretreatment; expression and surface localization of the mutant channels were unaffected by TCEP treatment. Co-expressed GFP was used as a loading control; the antibody consistently recognized two bands in our expression system. Data are representative of three independent experiments; *mock* indicates transfection with empty vector. *B*, schematic interpretation of results. The pore-associated mutated TM1 residue, F54C, interacts with the endogenous C-terminal Cys-426 via a disulfide bond, such that the C terminus remains in the pore even after it has been cut by TEVp. Channel inhibition by the cleaved hPANX1F54C channel can be relieved by disrupting the cysteine cross-link, either by using TCEP or by mutation of Cys-426, the interacting residue.

the C terminus, along with select residues in TM1, contributes to the channel pore (17). Because we observed that the isolated C terminus can inhibit truncated hPANX1 channels, we considered the possibility that the C-terminal inhibition may be mediated within the hPANX1 pore and that removal of the C terminus following cleavage would relieve such a block. If this were the case, locking the C terminus in the pore would yield a channel that was resistant to activation by this C-terminal cleavage mechanism, at least until the lock was broken.

To test this idea, we employed a reversible cysteine cross-linking paradigm focusing on residues identified as pore-associated in the previous study, specifically Phe-54 and Cys-426 (17); the phenylalanine is at the extracellular end of the predicted TM1 pore helix, and the endogenous cysteine is at the extreme C terminus. We found that incorporating an F54C mutation into the hPANX1(TEV) construct yielded a channel that was poorly activated by TEVp-mediated C-terminal cleavage (Fig. 4*A*). Consistent with the idea that the deficiency in channel activation reflects formation of a reversible disulfide involving the introduced cysteine, we showed that pretreatment with the reducing agent TCEP (500 μM) allowed cleavage-mediated activation of hPANX1(F54C). The TCEP-dependent activation of hPANX1(F54C) required prior cleavage of the C terminus because TCEP had no effect on hPANX1(F54C) channels in the absence of TEVp (Fig. 4*A*). To test whether F54C was interacting with the endogenous, pore-associated Cys-426 residue to interfere with cleavage-mediated activation, we generated the double mutant construct hPANX1(F54C/C426S). Indeed, in the absence of Cys-426, the F54C mutation was no longer able to interfere with cleavage-mediated channel activation, and pretreatment with TCEP did not further increase currents from the cleaved hPANX1(F54C/C426S) double mutant channel (Fig. 4*A*). These differences in current could not be explained by altered surface expression due to the mutations or treatment with TCEP because the channels appear equally well localized to the cell membrane under all conditions (Fig. 4*A*, *insets*). Together, these data suggest that dissociation of the C-terminal tail from the channel pore is required for activation of the channel following cleavage (Fig. 4*B*).

DISCUSSION

In this study, we examined how caspase-mediated C-terminal cleavage leads to hPANX1 channel activation, a mechanism that underlies release of ATP from cells undergoing apoptosis (5). We find that cleavage of the C terminus at the caspase site is sufficient to activate membrane-resident hPANX1 channels, without the need for additional apoptotic signals. The C terminus appears to function as a dissociable channel blocker because it is capable of inhibiting C-terminally truncated hPANX1 channels in *trans* and because the relief of C-terminal inhibition following cleavage does not occur if the C terminus is covalently tethered to the channel pore. Given these results, we propose a "ball-and-chain" mechanism for C-terminally mediated inhibition of hPANX1, with the caspase site being remarkably well placed to remove key determinants required for channel inhibition.

A ball-and-chain mechanism for channel inhibition is known classically from studies of inactivation of voltage-gated channels (18, 19). In more closely related connexin channels, the pH modulation of Cx47 (20, 21) and fast transjunctional voltage (Vj)-dependent gating of Cx40 and Cx43 (22, 23) have also been characterized as a ball-and-chain mechanism. In these cases, this type of mechanism was supported by showing that an isolated ball region could rescue inactivation, pH sensitivity, or Vj-dependent gating in truncated channels (24, 25). Likewise, we found that isolated C-terminal constructs can inhibit C-terminally truncated hPANX1 channels. Along with the earlier substituted cysteine accessibility method (SCAM) analysis that localized the C terminus to the pore (17) and our demonstration that dissociation of the C terminus from the channel pore is required for relief of hPANX1 inhibition, these findings lead us to favor a simple pore block model. Although our data cannot exclude the alternative possibility of an allosteric mechanism, they do imply that such a mechanism would require an interaction site for the C terminus within or near the pore. In other cases of ball-and-chain inhibition, there has been no physiological mechanism described for cutting the chain to permanently remove channel inhibition, as we have found for caspase-mediated cleavage and activation of hPANX1. Although this cleavage-based mechanism seems appropriate for a terminal process such as apoptosis, we expect that more subtle mechanisms will account for other forms of PANX1 activation associated with different physiological conditions (10, 26, 27). Nevertheless, because C-terminal inhibition in the intact channel depends on its association with the pore, our data suggest that these other PANX1 activation mechanisms will also require some disruption of the C terminus from its inhibitory interaction site within the channel pore.

We found that cleavage-mediated channel activation required removal of a critical region immediately downstream of the hPANX1 C-terminal caspase site that is divergent in mouse and human PANX1. Interestingly, although both mPanx1 and hPANX1 currents were strongly enhanced by cleavage at this caspase site, much of the difference in currents obtained with silent, full-length hPANX1 and basally active, full-length mPanx1 could be accounted for by variations in this downstream region. Of particular interest among the activating mutations we found in this region, a relatively modest substitution of hPANX1 to the corresponding mPanx1 residue (hPANX1A386L) yielded depolarization-activated currents that were approximately equivalent in magnitude to those of wild type mPanx1. It should be appreciated that more proximal C-terminal regions must also contribute to channel inhibition. For example, we found that a synthetic peptide containing just this sequence was not sufficient to block current from truncated hPANX1 channels, whereas larger C-terminal proteins were effective. In addition, a more proximal C-terminal residue (Cys-347) that regulates basal channel activity has been identified (16). It is also interesting that hPANX1 inhibition associated with mutations in this restricted region or obtained by cell-free reconstitution of C-terminal proteins with truncated channels was most pronounced at hyperpolarized potentials. The hPANX1 channel is inherently voltage-dependent (28), and the corresponding voltage dependence of C-terminal channel inhibition suggests that hPANX1 may adopt a conformation at depolarized potentials with which the C terminus interacts less avidly. Such a change in affinity may become especially noticeable when important binding determinants are mutated or, in the case of the isolated purified C terminus, when it is not tethered to the channel or perhaps fails to precisely mimic its native fold.

The mechanism we uncovered for hPANX1 channel regulation suggests some potential practical implications. For example, because cleavage-mediated hPANX1 activation can be functionally separated from apoptosis, it may be possible to use hPANX1(TEV) and an inducible TEVp system to study cellular consequences of hPANX1 activation and/or ATP release from nonapoptotic cells. Perhaps more importantly, the identification of this mechanism provides a promising inroad for development of compounds that could inhibit or activate hPANX1 by mimicking or blocking the inhibitory intramolecular interaction between the C terminus and the channel pore. Because hPANX1 appears to be critical for find-me signal release and prompt clearance of apoptotic cells (5), such compounds could find use in conditions where manipulation of cell clearance may be advantageous (*e.g.* autoimmune disease and cancer) (2, 29, 30).

Acknowledgements—We thank members of the Bayliss laboratory for advice and insights. We are grateful to Dr. G. S. Salvesen, who generously provided purified caspase 3, and Dr. S. R. Ikeda and Dr. T. E. Harris for TEVp and Spo20 expression constructs.

REFERENCES

1. MacVicar, B. A., and Thompson, R. J. (2010) Non-junction functions of pannexin 1 channels. *Trends Neurosci.* **33,** 93–102
2. D'hondt, C., Ponsaerts, R., De Smedt, H., Bultynck, G., and Himpens, B. (2009) Pannexins, distant relatives of the connexin family with specific cellular functions? *Bioessays.* **31,** 953–974
3. Sosinsky, G. E., Boassa, D., Dermietzel, R., Duffy, H. S., Laird, D. W., MacVicar, B., Naus, C. C., Penuela, S., Scemes, E., Spray, D. C., Thompson, R. J., Zhao, H. B., and Dahl, G. (2011) Pannexin channels are not gap junction hemichannels. *Channels* **5,** 193–197
4. Dubyak, G. R. (2009) Both sides now: multiple interactions of ATP with pannexin 1 hemichannels. Focus on "A permeant regulating its permeation pore: inhibition of pannexin 1 channels by ATP". *Am. J. Physiol. Cell*

Physiol. **296,** C235–C241
5. Chekeni, F. B., Elliott, M. R., Sandilos, J. K., Walk, S. F., Kinchen, J. M., Lazarowski, E. R., Armstrong, A. J., Penuela, S., Laird, D. W., Salvesen, G. S., Isakson, B. E., Bayliss, D. A., and Ravichandran, K. S. (2010) Pannexin 1 channels mediate "find-me" signal release and membrane permeability during apoptosis. *Nature* **467,** 863–867
6. Elliott, M. R., Chekeni, F. B., Trampont, P. C., Lazarowski, E. R., Kadl, A., Walk, S. F., Park, D., Woodson, R. I., Ostankovich, M., Sharma, P., Lysiak, J. J., Harden, T. K., Leitinger, N., and Ravichandran, K. S. (2009) Nucleotides released by apoptotic cells act as a find-me signal to promote phagocytic clearance. *Nature* **461,** 282–286
7. Bao, L., Locovei, S., and Dahl, G. (2004) Pannexin membrane channels are mechanosensitive conduits for ATP. *FEBS Lett.* **572,** 65–68
8. Silverman, W. R., de Rivero Vaccari, J. P., Locovei, S., Qiu, F., Carlsson, S. K., Scemes, E., Keane, R. W., and Dahl, G. (2009) The pannexin 1 channel activates the inflammasome in neurons and astrocytes. *J. Biol. Chem.* **284,** 18143–18151
9. Qiu, F., and Dahl, G. (2009) A permeant regulating its permeation pore: inhibition of pannexin 1 channels by ATP. *Am. J. Physiol. Cell Physiol.* **296,** C250–C255
10. Billaud, M., Lohman, A. W., Straub, A. C., Looft-Wilson, R., Johnstone, S. R., Araj, C. A., Best, A. K., Chekeni, F. B., Ravichandran, K. S., Penuela, S., Laird, D. W., and Isakson, B. E. (2011) Pannexin 1 regulates α1-adrenergic receptor-mediated vasoconstriction. *Circ. Res.* **109,** 80–85
11. Qu, Y., Misaghi, S., Newton, K., Gilmour, L. L., Louie, S., Cupp, J. E., Dubyak, G. R., Hackos, D., and Dixit, V. M. (2011) Pannexin 1 is required for ATP release during apoptosis but not for inflammasome activation. *J. Immunol.* **186,** 6553–6561
12. Denault, J. B., and Salvesen, G. S. (2008) Apoptotic caspase activation and activity. *Methods Mol. Biol.* **414,** 191–220
13. Williams, D. J., Puhl, H. L., 3rd, and Ikeda, S. R. (2009) Rapid modification of proteins using a rapamycin-inducible tobacco etch virus protease system. *PLoS One.* **4,** e7474
14. Su, W., Yeku, O., Olepu, S., Genna, A., Park, J. S., Ren, H., Du, G., Gelb, M. H., Morris, A. J., and Frohman, M. A. (2009) 5-Fluoro-2-indolyl deschlorohalopemide (FIPI), a phospholipase D pharmacological inhibitor that alters cell spreading and inhibits chemotaxis. *Mol. Pharmacol.* **75,** 437–446
15. Lei, Q., Talley, E. M., and Bayliss, D. A. (2001) Receptor-mediated inhibition of G protein-coupled inwardly rectifying potassium channels involves $G\alpha_q$ family subunits, phospholipase C, and a readily diffusible messenger. *J. Biol. Chem.* **276,** 16720–16730
16. Bunse, S., Schmidt, M., Prochnow, N., Zoidl, G., and Dermietzel, R. (2010) Intracellular cysteine 346 is essentially involved in regulating Panx1 channel activity. *J. Biol. Chem.* **285,** 38444–38452
17. Wang, J., and Dahl, G. (2010) SCAM analysis of Panx1 suggests a peculiar pore structure. *J. Gen. Physiol.* **136,** 515–527
18. Hoshi, T., Zagotta, W. N., and Aldrich, R. W. (1990) Biophysical and molecular mechanisms of Shaker potassium channel inactivation. *Science* **250,** 533–538
19. Armstrong, C. M., Bezanilla, F., and Rojas, E. (1973) Destruction of sodium conductance inactivation in squid axons perfused with pronase. *J. Gen. Physiol.* **62,** 375–391
20. Maeda, S., Nakagawa, S., Suga, M., Yamashita, E., Oshima, A., Fujiyoshi, Y., and Tsukihara, T. (2009) Structure of the connexin 26 gap junction channel at 3.5 Å resolution. *Nature* **458,** 597–602
21. Bargiello, T. A., Tang, Q., Oh, S., and Kwon, T. (2011) Voltage-dependent conformational changes in connexin channels. *Biochim. Biophys. Acta*, in press
22. Morley, G. E., Taffet, S. M., and Delmar, M. (1996) Intramolecular interactions mediate pH regulation of connexin43 channels. *Biophys. J.* **70,** 1294–1302
23. Moreno, A. P., Chanson, M., Elenes, S., Anumonwo, J., Scerri, I., Gu, H., Taffet, S. M., and Delmar, M. (2002) Role of the carboxyl terminal of connexin43 in transjunctional fast voltage gating. *Circ. Res.* **90,** 450–457
24. Ek-Vitorín, J. F., Calero, G., Morley, G. E., Coombs, W., Taffet, S. M., and Delmar, M. (1996) PH regulation of connexin43: molecular analysis of the gating particle. *Biophys. J.* **71,** 1273–1284
25. Zagotta, W. N., Hoshi, T., and Aldrich, R. W. (1990) Restoration of inactivation in mutants of Shaker potassium channels by a peptide derived from ShB. *Science* **250,** 568–571
26. Li, S., Bjelobaba, I., Yan, Z., Kucka, M., Tomic, M., and Stojilkovic, S. S. (2011) Expression and roles of pannexins in ATP release in the pituitary gland. *Endocrinology* **152,** 2342–2352
27. Seminario-Vidal, L., Okada, S. F., Sesma, J. I., Kreda, S. M., van Heusden, C. A., Zhu, Y., Jones, L. C., O'Neal, W. K., Penuela, S., Laird, D. W., Boucher, R. C., and Lazarowski, E. R. (2011) Rho signaling regulates pannexin 1-mediated ATP release from airway epithelia. *J. Biol. Chem.* **286,** 26277–26286
28. Ma, W., Hui, H., Pelegrin, P., and Surprenant, A. (2009) Pharmacological characterization of pannexin 1 currents expressed in mammalian cells. *J. Pharmacol. Exp. Ther.* **328,** 409–418
29. Chekeni, F. B., and Ravichandran, K. S. (2011) The role of nucleotides in apoptotic cell clearance: implications for disease pathogenesis. *J. Mol. Med.* **89,** 13–22
30. Lai, C. P., Bechberger, J. F., Thompson, R. J., MacVicar, B. A., Bruzzone, R., and Naus, C. C. (2007) Tumor-suppressive effects of pannexin 1 in C6 glioma cells. *Cancer Res.* **67,** 1545–1554